

Problem-free time-dependent variational principle for open quantum systems

Loïc Joubert-Doriol^{1,2} and Artur F. Izmaylov^{1,2}

¹*Department of Physical and Environmental Sciences, University of Toronto Scarborough, Toronto, Ontario, M1C 1A4, Canada*

²*Chemical Physics Theory Group, Department of Chemistry, University of Toronto, Toronto, Ontario M5S 3H6, Canada*

(Dated: 3 March 2022)

Methods of quantum nuclear wave-function dynamics have become very efficient in simulating large isolated systems using the time-dependent variational principle (TDVP). However, a straightforward extension of the TDVP to the density matrix framework gives rise to methods that do not conserve the energy in the isolated system limit and the total system population for open systems where only energy exchange with environment is allowed. These problems arise when the system density is in a mixed state and is simulated using an incomplete basis. Thus, the basis set incompleteness, which is inevitable in practical calculations, creates artificial channels for energy and population dissipation. To overcome this unphysical behavior, we have introduced a constrained Lagrangian formulation of TDVP applied to a non-stochastic open system Schrödinger equation (NOSSE) [L. Joubert-Doriol, I. G. Ryabinkin, and A. F. Izmaylov, *J. Chem. Phys.* **141**, 234112 (2014)]. While our formulation can be applied to any variational ansatz for the system density matrix, derivation of working equations and numerical assessment are done within the variational multiconfiguration Gaussian approach for a two-dimensional linear vibronic coupling model system interacting with a harmonic bath.

I. INTRODUCTION

Modelling photo-induced quantum dynamics in large molecular systems requires consideration of relatively localized chromophoric regions where this dynamics originates as well as macroscopic environment embedding these regions and influencing their behavior.¹⁻³ This is a very challenging task due to exponential scaling of quantum mechanics with the number of degrees of freedom (DOF).

One successful approach to reduce the prefactor of the exponential scaling for isolated systems in pure states is to project the time-dependent Schrödinger equation (TDSE) onto a time-dependent basis set. The basis time-dependence gives flexibility to minimize an error in an approximate solution of the TDSE with reduced computational cost as compared to that for static bases. Equations of motion (EOM) for the basis set parameters are obtained using the time-dependent variational principle (TDVP).⁴⁻⁶ This approach led to methods that are able to describe up to hundreds of nuclear DOF such as multi-configuration time-dependent Hartree (MCTDH) single-^{7,8} and multi-layer⁹ methods, as well as variational multiconfiguration Gaussian (vMCG) method.^{10,11} However, computational costs of these approaches still scale exponentially with the number of DOF so that molecular systems such as proteins (several thousands of DOF) cannot be simulated yet. Moreover, wave-function methods cannot describe energy dissipation and quantum decoherence of a system interacting with environment in a mixed state (e.g., heat reservoir or incoherent sun light¹²) without departing from the TDSE.¹³

The quantum master equation (QME) formalism involving the system density matrix (DM) can model interaction of the quantum system with large macroscopic environment and describe associated processes of energy

exchange and quantum decoherence.^{13,14} These processes give rise to mixed states of the quantum system, which cannot be described with a single wave-function. Therefore, the use of a DM, $\hat{\rho}(t)$, becomes indispensable, and the TDSE is replaced by the QME

$$\dot{\hat{\rho}}(t) = \mathcal{L}[\hat{\rho}(t)], \quad (1)$$

where the dot stands for the partial time derivative, and \mathcal{L} is the Liouvillian super-operator. In the case of an isolated system with the Hamiltonian \hat{H} ,

$$\mathcal{L}[\hat{\rho}(t)] = -i[\hat{H}, \hat{\rho}(t)], \quad (2)$$

and Eq. (1) becomes the Liouville-von Neumann equation that generates a unitary evolution of the DM in which the system energy is conserved. For an open system, \mathcal{L} also contains a non-unitary part that is responsible for energy dissipation and quantum decoherence. This non-unitary part is obtained either from purely mathematical reasoning to preserve semi-positivity of the system density (e.g., Lindblad approach¹⁵) or derived using perturbation theory with respect to the system-bath coupling, Redfield¹⁶, Caldeira-Legett¹⁷, and time-convolutionless formulations. All these formulations reduce environmental effects to few terms in \mathcal{L} that contain only the system DOF, hence, excluding environmental DOF from the explicit consideration. This reduction employs perturbative consideration of system-environment interaction and thus is adequate only for weak system-environment couplings.

Practical necessity to have small system-bath couplings usually requires to consider a large number of system DOF in the QME framework, and thus, it increases the computational cost of simulation. Therefore, use of a time-dependent basis guided by the TDVP for simulating system dynamics in the QME approach seems as an

ideal choice for modelling large open systems. Combining the TDVP with QME has been attempted in the past, [8,18,19](#) however, these attempts revealed that resulting dynamical equations exhibit unphysical behavior which was traced to basis set incompleteness. The first problem is non-conservation of the DM trace, $\text{Tr}\{\dot{\hat{\rho}}(t)\} \neq 0$, for open systems where only the energy but not the matter exchange is allowed. [18,20](#) The second problem is violation of energy conservation for an isolated system in a mixed state, [6,20,21](#) $\text{Tr}\{\dot{\hat{\rho}}(t)\hat{H}\} \neq 0$. It is important to note that in the context of the McLachlan TDVP for wavefunctions, to conserve the energy, there is a requirement for a wave-function to be analytic with respect to variational parameters. This requirement makes the McLachlan TDVP [6](#) equivalent to a principle of least action [22](#) that guarantees the energy conservation. [23](#) However, violation of the energy conservation in the density formalism has a different origin and takes place even if the density parameterization is analytic. It appears as a result of the DM entering quadratically in the TDVP, which makes $\text{Tr}\{\hat{\rho}(t)^2\hat{H}\}$ a conserved quantity [20](#) rather than the energy $E = \text{Tr}\{\hat{\rho}(t)\hat{H}\}$.

These two problems create artificial channels of population and energy flows that can lead to inadequate results. A straightforward solution involving corresponding constraints imposed through the Lagrange multiplier method [21](#) does not preserve a unitary character of quantum dynamics in the isolated system limit. [24](#) This can lead to more subtle artifacts such as non-conservation of the density matrix purity ($\text{Tr}\{\hat{\rho}^2\}$). Another, so-called linear mean-field approach has been suggested by Raab *et al.* [19](#) within the MCTDH framework to resolve these issues. However, this method becomes non-variational for open systems.

The aim of this paper is to resolve the non-conservation problems using a hybrid approach: To address the energy non-conservation problem in isolated systems we apply the TDVP not to the QME equation but to its recently developed equivalent, non-stochastic open system Schrödinger equation (NOSSE) [25](#). NOSSE does not have issues with energy conservation within the TDVP framework because it is formulated with respect to a square root of the density. The root square dynamics is unitary for an isolated system and allows for the full reconstruction of the system density matrix evolution by evaluating the square at each time. The trace non-conservation occurs only for open systems in TDVP NOSSE formulation and is resolved by imposing conservation of the trace of the density matrix through a Lagrangian multiplier. This constraint does not interfere with the unitarity of dynamics in the isolated system limit and thus does not introduce any artifacts.

The rest of the paper is organized as follows. Section [II](#) is devoted to exposing the non-conservation problems at the formal level and details our solutions. Section [III](#) provides numerical examples illustrating performance of our TDVP on a model system. Section [IV](#) concludes this paper and gives an overview of future work.

II. THEORY

A. TDVP problems in the density matrix formalism

We start by illustrating formally origins of the TDVP problems in the density matrix formalism. We introduce a finite linear subspace \mathcal{S} of the total Hilbert space that contains time-dependent, not necessarily orthonormal, basis functions $\{|\varphi_k(t)\rangle; k = 1, \dots, N_b\}$. A projector on \mathcal{S} is built as $\hat{P}_{N_b}(t) = \sum_{kl} |\varphi_k(t)\rangle [\mathbf{S}^{-1}(t)]_{kl} \langle \varphi_l(t)|$, where $S_{kl}(t) = \langle \varphi_k(t) | \varphi_l(t) \rangle$ is an element of the overlap matrix. The time dependency of the $|\varphi_k(t)\rangle$ is given through sets of parameters $z_{\alpha k}(t)$, where the Greek subscript labels different parameters corresponding to the same basis function. Our only requirement on the parameterization of the basis is the analyticity condition [22](#)

$$\frac{\partial |\varphi_k(t)\rangle}{\partial z_{\alpha k}^*(t)} = 0, \quad (3)$$

so that the parameterization preserves the energy in the limiting case of an isolated system in a pure state.

In the time-dependent basis, $\hat{\rho}(t)$ is expressed as

$$\hat{\rho}(t) = \sum_{kl} |\varphi_k(t)\rangle B_{kl}(t) \langle \varphi_l(t)|, \quad (4)$$

where $B_{lk}(t)$ are time-dependent, Hermitian [$B_{kl}(t) = B_{lk}(t)^*$] coefficients. For notational simplicity, when it is not essential, the time argument will be skipped in the further consideration. A straightforward extension of the McLachlan TDVP to the density formalism involves minimization of the Frobenius norm of the error

$$\|\dot{\hat{\rho}} - \mathcal{L}[\hat{\rho}]\| = \text{Tr}\{(\dot{\hat{\rho}} - \mathcal{L}[\hat{\rho}])^\dagger (\dot{\hat{\rho}} - \mathcal{L}[\hat{\rho}])\}^{1/2}, \quad (5)$$

which is equivalent to satisfying a stationary condition [20](#)

$$\text{Tr}\left\{\delta\hat{\rho}\left(\dot{\hat{\rho}} - \mathcal{L}[\hat{\rho}]\right)\right\} = 0. \quad (6)$$

Replacing $\hat{\rho}$ by Eq. (4) in Eq. (6) we obtain EOM for $\mathbf{B} = \{B_{kl}\}$ and $z_{\alpha k}$ (detailed derivation is given in App. [V](#))

$$\dot{\mathbf{B}} = \mathbf{S}^{-1} \mathbf{L} \mathbf{S}^{-1} - (\mathbf{S}^{-1} \boldsymbol{\tau} \mathbf{B} + \mathbf{B} \boldsymbol{\tau}^\dagger \mathbf{S}^{-1}), \quad (7)$$

$$\sum_{\beta l} \tilde{C}_{kl}^{\alpha\beta} \dot{z}_{\beta l} = \tilde{Y}_k^\alpha, \quad (8)$$

where $[\boldsymbol{\tau}]_{kl} = \langle \varphi_k | \dot{\varphi}_l \rangle$, $[\mathbf{L}]_{kl} = \langle \varphi_k | \mathcal{L}[\hat{\rho}] | \varphi_l \rangle$, and

$$\tilde{C}_{kl}^{\alpha\beta} = \left\langle \frac{\partial \varphi_k}{\partial z_{\alpha k}} \left[\left[\hat{1} - \hat{P}_{N_b} \right] \left| \frac{\partial \varphi_l}{\partial z_{\beta l}} \right. \right] \right\rangle [\mathbf{B} \mathbf{S} \mathbf{B}]_{lk}, \quad (9)$$

$$\tilde{Y}_k^\alpha = \sum_l \left\langle \frac{\partial \varphi_k}{\partial z_{\alpha k}} \left[\left[\hat{1} - \hat{P}_{N_b} \right] \mathcal{L}[\hat{\rho}] \left| \varphi_l \right. \right] \right\rangle B_{lk}. \quad (10)$$

Equation (8) is solved for $\dot{\mathbf{z}} = \{\dot{z}_{\alpha k}\}$ as a linear equation where $\dot{\mathbf{z}}$ and $\tilde{\mathbf{Y}}$ are vectors and $\tilde{\mathbf{C}}$ is a matrix

$$\dot{\mathbf{z}} = \tilde{\mathbf{C}}^{-1} \tilde{\mathbf{Y}}. \quad (11)$$

A given parameterization can lead to redundancies between some of the parameters $z_{\alpha k}$ and B_{kl} (e.g., in the

MCTDH and vMCG methods). In such cases extra relations between redundant parameters must be combined with Eqs. (7) and (11) to eliminate any redundancies.

Equations (7) and (11) are equivalent to EOM obtained in the particular case of moving Gaussians derived in Ref. 8. This is not fortuitous since the ‘‘type II’’ density parameterization of Ref. 8 coincides with that of Eq. (4). By choosing the MCTDH ansatz for the time-dependent basis, it can be verified that Eqs. (7)-(11) provide the EOM obtained in Refs. 19 and 20 (up to the removal of redundancies in parameterization).

To illustrate variation of the total system population we will use the derived EOM to consider time derivative of the system population

$$\text{Tr}\{\dot{\rho}(t)\} = \text{Tr}\{\dot{\mathbf{B}}\mathbf{S} + (\boldsymbol{\tau} + \boldsymbol{\tau}^\dagger)\mathbf{B}\}. \quad (12)$$

Using Eq. (7) the variation of the DM trace on time is given by

$$\begin{aligned} \text{Tr}\{\dot{\rho}(t)\} &= \text{Tr}\{\mathbf{S}^{-1}\mathbf{L} - \mathbf{S}^{-1}\boldsymbol{\tau}\mathbf{B}\mathbf{S} - \mathbf{B}\boldsymbol{\tau}^\dagger + (\boldsymbol{\tau} + \boldsymbol{\tau}^\dagger)\mathbf{B}\} \\ &= \text{Tr}\{\mathbf{S}^{-1}\mathbf{L}\} = \text{Tr}\{\hat{P}_{N_b}\mathcal{L}[\hat{\rho}]\}, \end{aligned} \quad (13)$$

where in the second equality we have used cyclic invariance and linearity of the trace operator. For incomplete bases $\hat{P}_{N_b}\mathcal{L}[\hat{\rho}] \neq \mathcal{L}[\hat{\rho}]$, and even if $\text{Tr}\{\mathcal{L}[\hat{\rho}]\} = 0$, $\text{Tr}\{\hat{P}_{N_b}\mathcal{L}[\hat{\rho}]\}$ can be non-zero for open systems as has been shown by Raab *et al.* for the Liouvillian in the Lindblad form.²⁰ In contrast, for isolated systems the population is always conserved because

$$\begin{aligned} \text{Tr}\{\hat{P}_{N_b}\mathcal{L}[\hat{\rho}]\} &= -i \text{Tr}\{\mathbf{S}^{-1}(\mathbf{H}\mathbf{B}\mathbf{S} - \mathbf{S}\mathbf{B}\mathbf{H})\} \\ &= -i \text{Tr}\{[\mathbf{H}, \mathbf{B}]\} = 0, \end{aligned} \quad (14)$$

where $[\mathbf{H}]_{kl} = \langle \varphi_k | \hat{H} | \varphi_l \rangle$.

For an isolated system, the energy variation with time is given by

$$\begin{aligned} \text{Tr}\{\dot{\rho}\hat{H}\} &= \text{Tr}\{\dot{\mathbf{B}}\mathbf{H} + \mathbf{B}\dot{\mathbf{H}}\} \\ &= \text{Tr}\{\dot{\mathbf{H}}\mathbf{B} - \mathbf{B}\mathbf{H}\mathbf{S}^{-1}\boldsymbol{\tau} - \boldsymbol{\tau}^\dagger\mathbf{S}^{-1}\mathbf{H}\mathbf{B}\}, \end{aligned} \quad (15)$$

where in the second equality we used the $\dot{\mathbf{B}}$ definition from Eq. (7), $[\dot{\mathbf{H}}]_{kl} = \langle \dot{\varphi}_k | \hat{H} | \varphi_l \rangle + \langle \varphi_k | \dot{\hat{H}} | \varphi_l \rangle$, and cyclic invariance of trace. Equation (15) can be further simplified using hermiticity of \mathbf{B} , \mathbf{H} , and \mathbf{S}

$$\begin{aligned} \text{Tr}\{\dot{\rho}\hat{H}\} &= \sum_{\alpha kl} 2 \text{Re} \left[\dot{z}_{\alpha k}^* \left\langle \frac{\partial \varphi_k}{\partial z_{\alpha k}} \left[[\hat{1} - \hat{P}_{N_b}] \hat{H} | \varphi_l \right] B_{lk} \right\rangle \right] \\ &= -2 \text{Im}[\text{Tr}\{\dot{\mathbf{z}}^\dagger \mathbf{Y}\}], \end{aligned} \quad (16)$$

where

$$[\mathbf{Y}]_k^\alpha = -i \sum_l \left\langle \frac{\partial \varphi_k}{\partial z_{\alpha k}} \left[[\hat{1} - \hat{P}_{N_b}] \hat{H} | \varphi_l \right] B_{lk} \right\rangle. \quad (17)$$

Using Eq. (11) and the vector notation for $\dot{\mathbf{z}}$ and \mathbf{Y} we arrive at

$$\text{Tr}\{\dot{\rho}\hat{H}\} = -2 \text{Im}[\tilde{\mathbf{Y}}^\dagger \tilde{\mathbf{C}}^{-1} \mathbf{Y}], \quad (18)$$

Equation (10) simplifies for isolated system to

$$\tilde{Y}_k^\alpha = -i \sum_l \left\langle \frac{\partial \varphi_k}{\partial z_{\alpha k}} \left[[\hat{1} - \hat{P}_{N_b}] \hat{H} | \varphi_l \right] [\mathbf{B}\mathbf{S}\mathbf{B}]_{lk} \right\rangle. \quad (19)$$

According to Eqs. (16) and (18), energy conservation takes place at least in four special cases:

1. Time-independent bases, where $\dot{\mathbf{z}} = 0$.
2. Complete bases, where $\hat{P}_{N_b} = \hat{1}$, and therefore, $\mathbf{Y} = 0$.
3. Systems in pure states, where $\mathbf{B}\mathbf{S}\mathbf{B} = \mathbf{B}$ (the idempotency condition), then $\tilde{\mathbf{Y}} = \mathbf{Y}$ and using hermiticity of $\tilde{\mathbf{C}}$, it is easy to see that $\text{Im}[\tilde{\mathbf{Y}}^\dagger \tilde{\mathbf{C}}^{-1} \mathbf{Y}] = \text{Im}[\mathbf{Y}^\dagger \tilde{\mathbf{C}}^{-1} \mathbf{Y}] = 0$.
4. Linear parameterization, $|\varphi_k\rangle = \sum_\alpha |\phi_\alpha\rangle z_{\alpha k}$, where $|\phi_\alpha\rangle$ are time-independent basis functions. In this case, Eq. (8) becomes $\mathbf{C}_0 \dot{\mathbf{z}} \mathbf{B}\mathbf{S}\mathbf{B} = \mathbf{Y}_0 \mathbf{B}\mathbf{S}\mathbf{B}$, where $[\mathbf{C}_0]_{\alpha\beta} = \langle \phi_\alpha | [\hat{1} - \hat{P}_{N_b}] | \phi_\beta \rangle$ and $[\mathbf{Y}_0]_{\alpha l} = \langle \phi_\alpha | [\hat{1} - \hat{P}_{N_b}] \hat{H} | \varphi_l \rangle$, which leads to $\dot{\mathbf{z}} = \mathbf{C}_0^{-1} \mathbf{Y}_0$, and similarly $\mathbf{Y} = \mathbf{Y}_0 \mathbf{B}$. Equation (16) gives $-2 \text{Im}[\text{Tr}\{\dot{\mathbf{z}}^\dagger \mathbf{Y}\}] = -2 \text{Im}[\text{Tr}\{\mathbf{Y}_0^\dagger \mathbf{C}_0^{-1} \mathbf{Y}_0 \mathbf{B}\}] = 0$, where we used hermiticity of \mathbf{C}_0 and \mathbf{B} , and semi-positivity of \mathbf{B} .

We would like to conclude this section by emphasizing that a general non-linear time-dependent parameterization (e.g., used in MCTDH and vMCG methods) of the density matrix will not conserve energy of the isolated system in a mixed state.

B. Constrained TDVP for NOSSE

To resolve the non-conservation problems we will use a problem specific approach: The population non-conservation for open system will be corrected by introducing a constraint using Lagrange multiplier method. For the problem of energy non-conservation we reformulate dynamical equations using non-stochastic Schrödinger equation for a square root of the density. This difference in approaches to the two problems stems from an objective to preserve unitarity of the dynamics in the isolated system limit. Imposing a constraint ensuring energy conservation breaks the unitarity of the isolated system dynamics and may lead to artifacts.²⁴

To proceed to formulation of EOM for a density square root in open systems, we introduce some notation first. Matrix \mathbf{B} is semi-positive, and therefore, there exist a matrix \mathbf{M} such that $\mathbf{B} = \mathbf{M}\mathbf{M}^\dagger$. Defining

$$|m_k\rangle = \sum_l |\varphi_l\rangle M_{lk}, \quad (20)$$

and using Eq. (4), we can rewrite the density matrix as

$$\begin{aligned}\hat{\rho} &= \sum_{abk} |\varphi_a\rangle M_{ak} M_{bk}^* \langle \varphi_b| \\ &= \sum_k |m_k\rangle \langle m_k|. \end{aligned} \quad (21)$$

All states $\{|m_k\rangle\}$ can be arranged in a vector form $\mathbf{m} = (|m_1\rangle |m_2\rangle \dots)$, such that \mathbf{m} represents a density square root because $\hat{\rho} = \mathbf{m}\mathbf{m}^\dagger$. In Ref. 25 we found EOM for \mathbf{m} for a system with a given Liouvillian operator \mathcal{L}

$$\dot{\mathbf{m}} = \mathcal{K}[\mathbf{m}], \quad (22)$$

where $\mathcal{K}[\mathbf{m}]$ is a vector of states that satisfies a Sylvester equation

$$\mathcal{K}[\mathbf{m}]\mathbf{m}^\dagger + \mathbf{m}\mathcal{K}[\mathbf{m}]^\dagger = \mathcal{L}[\mathbf{m}\mathbf{m}^\dagger]. \quad (23)$$

Note that for an isolated system $\mathcal{K}[\mathbf{m}]$ reduces to $-iH\mathbf{m}$ and Eq. (22) becomes an uncoupled set of TDSE for each component of \mathbf{m} . This reduction guarantees that application of TDVP to Eq. (22) will be free from energy conservation issues arising in the density formalism. In order to optimize the parameters of \mathbf{m} , the Frobenius norm $\|\dot{\mathbf{m}} - \mathcal{K}[\mathbf{m}]\|$ is minimized.

To address non-conservation of the total population for open systems we introduce a corresponding constraint using the Lagrange multiplier method. The Lagrangian function is

$$\Lambda = \|\dot{\mathbf{m}} - \mathcal{K}[\mathbf{m}]\|^2 + \lambda \frac{\partial}{\partial t} \text{Tr}\{\mathbf{m}\mathbf{m}^\dagger\}, \quad (24)$$

where λ is a Lagrange multiplier. Minimizing Λ with respect to parameters $\mathbf{M} = \{M_{kl}\}$, \mathbf{z} , and λ leads to a constrained TDVP

$$\text{Re} [\text{Tr} \{ \delta \dot{\mathbf{m}}^\dagger (\dot{\mathbf{m}} - \mathcal{K}[\mathbf{m}] + \lambda \mathbf{m}) \}] = 0, \quad (25)$$

$$\frac{\partial}{\partial t} \text{Tr}\{\mathbf{m}\mathbf{m}^\dagger\} = 0. \quad (26)$$

Replacing \mathbf{m} by its explicit form [Eq. (20)] in Eq. (25) and Eq. (26) we obtain EOM for \mathbf{M} and \mathbf{z} (details of the derivation are given in App. VI)

$$\begin{aligned}\dot{\mathbf{M}} &= \mathbf{S}^{-1}\mathbf{K} - \mathbf{S}^{-1}\boldsymbol{\tau}\mathbf{M} \\ &\quad - \frac{1}{2} \text{Tr}\{\mathbf{K}\mathbf{M}^\dagger + \mathbf{M}\mathbf{K}^\dagger\}\mathbf{M} \end{aligned} \quad (27)$$

$$\dot{\mathbf{z}} = \mathbf{C}^{-1}\mathbf{Y}, \quad (28)$$

where $K_{kl} = \langle \varphi_k | \mathcal{K}_l[\mathbf{m}] \rangle$ and

$$C_{kl}^{\alpha\beta} = \left\langle \frac{\partial \varphi_k}{\partial z_{\alpha k}} \left[\left[\hat{1} - \hat{P}_{N_b} \right] \left| \frac{\partial \varphi_l}{\partial z_{l\beta}} \right. \right] [\mathbf{M}\mathbf{M}^\dagger]_{lk}, \quad (29)$$

$$Y_k^\alpha = \sum_l \left\langle \frac{\partial \varphi_k}{\partial z_{\alpha k}} \left[\left[\hat{1} - \hat{P}_{N_b} \right] |[\mathcal{K}_l[\mathbf{m}]\rangle M_{kl}^* \right. \right. \quad (30)$$

Using the relation $\dot{\mathbf{B}} = \dot{\mathbf{M}}\mathbf{M}^\dagger + \mathbf{M}\dot{\mathbf{M}}^\dagger$, Eq. (27) can be recast into an EOM for \mathbf{B}

$$\dot{\mathbf{B}} = \mathbf{S}^{-1}\mathbf{L}\mathbf{S}^{-1} - (\mathbf{S}^{-1}\boldsymbol{\tau}\mathbf{B} + \mathbf{B}\boldsymbol{\tau}^\dagger\mathbf{S}^{-1}) - \text{Tr}\{\mathbf{S}^{-1}\mathbf{L}\}\mathbf{B}, \quad (31)$$

where we employed the Sylvester equation [Eq. (23)] in the matrix form, $\mathbf{L} = \mathbf{K}\mathbf{M}^\dagger\mathbf{S} + \mathbf{S}\mathbf{M}\mathbf{K}^\dagger$.

Now, it is easy to show that Eqs. (28-31) conserve all required quantities. Taking the trace of $\dot{\hat{\rho}} = \frac{\partial}{\partial t} \sum_{kl} |\varphi_k\rangle B_{kl} \langle \varphi_l|$ and using Eq. (31) gives

$$\begin{aligned}\frac{\partial}{\partial t} \text{Tr}\{\hat{\rho}\} &= \text{Tr}\{\dot{\mathbf{B}}\mathbf{S} + (\boldsymbol{\tau} + \boldsymbol{\tau}^\dagger)\mathbf{B}\} \\ &= \text{Tr}\{\mathbf{S}^{-1}\mathbf{L} - \text{Tr}\{\mathbf{S}^{-1}\mathbf{L}\}\mathbf{B}\mathbf{S}\} = 0, \end{aligned} \quad (32)$$

where the last equality holds since $\text{Tr}\{\hat{\rho}\} = \text{Tr}\{\mathbf{B}\mathbf{S}\} = 1$. Therefore, the trace is conserved for any Liouvillian $\mathcal{L}[\hat{\rho}]$. If the system is isolated, $\mathcal{L}[\hat{\rho}] = -i[\hat{H}, \hat{\rho}]$ in Eq. (31), it is possible to show that a trace of any power of $\hat{\rho}$ is also conserved

$$\begin{aligned}\frac{\partial}{\partial t} \text{Tr}\{\hat{\rho}^n\} &= \text{Tr}\{\dot{\mathbf{B}}\mathbf{S}(\mathbf{B}\mathbf{S})^{n-1} + \mathbf{B}(\boldsymbol{\tau} + \boldsymbol{\tau}^\dagger)(\mathbf{B}\mathbf{S})^{n-1}\} \\ &= -i \text{Tr}\{\mathbf{S}^{-1}(\mathbf{H}\mathbf{B}\mathbf{S} - \mathbf{S}\mathbf{B}\mathbf{H})(\mathbf{B}\mathbf{S})^{n-1} \\ &\quad - \text{Tr}\{\mathbf{S}^{-1}(\mathbf{H}\mathbf{B}\mathbf{S} - \mathbf{S}\mathbf{B}\mathbf{H})\}(\mathbf{B}\mathbf{S})^n\} = 0. \end{aligned} \quad (33)$$

This illustrates unitary character of dynamics. The energy is also conserved for the isolated system limit

$$\begin{aligned}\frac{\partial}{\partial t} \text{Tr}\{\hat{\rho}\hat{H}\} &= \text{Tr}\{\dot{\mathbf{B}}\mathbf{H} + \mathbf{B}\dot{\mathbf{H}}\} \\ &= \text{Tr}\{\mathbf{B}\dot{\mathbf{H}} - \mathbf{S}^{-1}\boldsymbol{\tau}\mathbf{B}\mathbf{H} - \mathbf{H}\mathbf{B}\boldsymbol{\tau}^\dagger\mathbf{S}^{-1}\} \\ &= -2 \text{Im}[\mathbf{z}^\dagger\mathbf{Y}] = -2 \text{Im}[\mathbf{Y}^\dagger\mathbf{C}^{-1}\mathbf{Y}] = 0, \end{aligned} \quad (34)$$

where we invoke the hermiticity of \mathbf{C} to see that $\mathbf{Y}^\dagger\mathbf{C}^{-1}\mathbf{Y}$ does not have imaginary component.

III. NUMERICAL EXAMPLES

A. Model

To illustrate performance of our developments for the case where system quantum effects are affected by interaction with environment, we will consider the simplest linear vibronic coupling (LVC) model²⁶ of crossing surfaces.^{27,28} The system contains two electronic states, donor $|D\rangle$ and acceptor $|A\rangle$, which are coupled through two nuclear DOF

$$\begin{aligned}\hat{H} &= \sum_{\alpha=1}^2 \frac{\omega_\alpha}{2} (\hat{p}_\alpha^2 + \hat{x}_\alpha^2) \left[|D\rangle \langle D| + |A\rangle \langle A| \right] \\ &\quad - d\hat{x}_1 \left[|D\rangle \langle D| - |A\rangle \langle A| \right] + c\hat{x}_2 \left[|D\rangle \langle A| + |A\rangle \langle D| \right], \end{aligned} \quad (35)$$

where ω_α is the frequency of the coordinate x_α , and d and c are diabatic coupling constants. Numerical values of the parameters are taken from Ref. 29 for the two-dimensional model of the bis(methylene) adamantyl radical cation: $\omega_1 = 7.743 \cdot 10^{-3}$ a.u., $\omega_2 = 6.680 \cdot 10^{-3}$ a.u., $d = 5.289 \cdot 10^{-3}$ a.u., $c = 9.901 \cdot 10^{-4}$ a.u. The dissipative part is introduced through bilinear coupling of the system coordinates x_α with coordinates of harmonic bath oscillators. System-bath couplings are taken small

enough so that the second order perturbation theory can be applied for the system-bath interaction in conjunction with the rotating wave and Markovian approximations. The resulting Liouvillian^{30,31} has a Lindblad form¹⁵

$$\begin{aligned} \mathcal{L}[\hat{\rho}] = & -i[\hat{H}, \hat{\rho}] + h_1 \sum_{\alpha=1}^2 \left(2\hat{Z}_\alpha \hat{\rho} \hat{Z}_\alpha^\dagger - \hat{Z}_\alpha^\dagger \hat{Z}_\alpha \hat{\rho} - \hat{\rho} \hat{Z}_\alpha^\dagger \hat{Z}_\alpha \right) \\ & + h_2 \sum_{\alpha=1}^2 \left(2\hat{Z}_\alpha^\dagger \hat{\rho} \hat{Z}_\alpha - \hat{Z}_\alpha \hat{Z}_\alpha^\dagger \hat{\rho} - \hat{\rho} \hat{Z}_\alpha \hat{Z}_\alpha^\dagger \right), \end{aligned} \quad (36)$$

where h_1 and h_2 are parameters that depend on the bath temperature, and \hat{Z}_α operators are defined as

$$\begin{aligned} \hat{Z}_1 &= \left(\hat{a}_1 - \frac{d}{\omega_1 \sqrt{2}} \right) |D\rangle \langle D| + \left(\hat{a}_1 + \frac{d}{\omega_1 \sqrt{2}} \right) |A\rangle \langle A| \\ \hat{Z}_2 &= \hat{a}_2 \left(|D\rangle \langle D| + |A\rangle \langle A| \right), \end{aligned} \quad (37)$$

with annihilation operators $\hat{a}_\alpha = (\hat{x}_\alpha + i\hat{p}_\alpha)/\sqrt{2}$. For $\mathcal{L}[\hat{\rho}]$ in the Lindblad form, $\mathcal{K}[\mathbf{m}]$ is derived in Ref. 25, and for our model is given by

$$\begin{aligned} \mathcal{K}[\mathbf{m}] = & -i\hat{H}\mathbf{m} + h_1 \sum_{\alpha=1}^2 \left(\hat{Z}_\alpha \hat{\rho} \hat{Z}_\alpha^\dagger (\mathbf{m}^\dagger)^{-1} - \hat{Z}_\alpha^\dagger \hat{Z}_\alpha \mathbf{m} \right) \\ & + h_2 \sum_{\alpha=1}^2 \left(\hat{Z}_\alpha^\dagger \hat{\rho} \hat{Z}_\alpha (\mathbf{m}^\dagger)^{-1} - \hat{Z}_\alpha \hat{Z}_\alpha^\dagger \mathbf{m} \right). \end{aligned} \quad (38)$$

B. Numerical details

We apply our constrained TDVP to the variational multiconfiguration Gaussian (vMCG) ansatz.¹⁰ In vMCG, the time-dependent basis consist of products

$$|\varphi_k\rangle = |\sigma_k\rangle |g_k\rangle \quad (39)$$

of discrete electronic parts $|\sigma_k\rangle = |D\rangle, |A\rangle$ and spatial two-dimensional moving Gaussian parts $|g_k\rangle$ parametrized as follows

$$\langle \mathbf{x} | g_k \rangle = \exp(-\mathbf{x}^T \mathbf{A}_k \mathbf{x} + \boldsymbol{\xi}_k^T \mathbf{x}), \quad (40)$$

where \mathbf{x} is a vector of the mass- and frequency-weighted nuclear coordinates, \mathbf{A}_k are frozen widths ($\dot{\mathbf{A}}_k = 0$) and $\boldsymbol{\xi}_k$ are parameters encoding the position ($\text{Re}[\boldsymbol{\xi}_k]$) and momentum ($\text{Im}[\boldsymbol{\xi}_k]$) of a Gaussian. This choice of parameterization satisfy the analyticity condition $\partial |\varphi_k\rangle / \partial \xi_{k\alpha}^* = 0$.

For reasons of numerical stability it is more convenient to work with coherent states (CSs) of harmonic oscillators rather than frozen Gaussians.^{11,32} However, EOM derived from the McLachlan TDVP expressions for CSs can have energy conservation issues because CSs do not satisfy the analyticity condition. On the other hand, TDVP EOM for frozen Gaussians can be projected onto the basis of CSs, $\{|z_k\rangle\}$, of harmonic oscillators with frequencies ω_α by multiplying Eq. (40) with $V_{kk} = e^{-\boldsymbol{\xi}_k^T \text{Re}[\boldsymbol{\xi}_k]/2}/\pi$ and setting $\mathbf{A}_k = \mathbf{1}_2/2$. The transformation of Gaussians

$|z_k\rangle = V_{kk} |g_k\rangle$ leads to a transformation of the matrix $\mathbf{B} = \mathbf{V} \mathbf{B} \mathbf{V}^\dagger$, where $[\mathbf{V}]_{kl} = V_{kk} \delta_{kl}$. In the CS representation variational parameters become $z_{\alpha k} = \xi_{k\alpha}/\sqrt{2}$, they correspond to eigenvalues of the annihilation operator \hat{a}_α for CSs $|z_k\rangle$

$$\hat{a}_\alpha |z_k\rangle = z_{\alpha k} |z_k\rangle. \quad (41)$$

Upon the \mathbf{V} transformation, the structure of the Eqs. (28-31) remains the same, thus, we will use these equations to propagate parameters of CSs.

The population loss for an open system is given by Eq. (13). In the particular case of the Liouvillian defined by Eq. (36) in the basis of CSs, the expression for the population loss becomes

$$\begin{aligned} \text{Tr}\{\dot{\hat{\rho}}\} = & 2 \sum_{\alpha=1}^2 \text{Tr}\{[h_1 \hat{Z}_\alpha^\dagger (\hat{P}_{N_b} - 1) \hat{Z}_\alpha \\ & + h_2 \hat{Z}_\alpha (\hat{P}_{N_b} - 1) \hat{Z}_\alpha^\dagger] \hat{\rho}\}. \end{aligned} \quad (42)$$

Equation (42) can be further simplified using the definitions of \hat{Z}_α [Eq. (37)], $\hat{\rho}$ [Eq. (4)], \hat{P}_{N_b} , and applying Eq. (41)

$$\begin{aligned} \text{Tr}\{\dot{\hat{\rho}}\} = & 2h_2 \sum_{\alpha=1}^2 \text{Tr}_N\{ \hat{a}_\alpha (\hat{P}_{N_b} - 1) \hat{a}_\alpha^\dagger \\ & \times [\langle D | \hat{\rho} | D \rangle + \langle A | \hat{\rho} | A \rangle] \}, \end{aligned} \quad (43)$$

where $\text{Tr}_N\{\dots\}$ is the trace over system nuclear DOF. Thus, the h_1 containing term disappears and the population loss takes place only if $h_2 \neq 0$.

The initial system DM $\hat{\rho}$ is taken as a Boltzmann distribution $\hat{\rho}_B$ in the donor electronic state

$$\hat{\rho}_B = \frac{e^{-\hat{P}_D \hat{H} \hat{P}_D / k_B T} \hat{P}_D}{\text{Tr}\{e^{-\hat{P}_D \hat{H} \hat{P}_D / k_B T} \hat{P}_D\}}, \quad (44)$$

where $\hat{P}_D = |D\rangle \langle D|$ is the projector on the donor electronic state, k_B is the Boltzmann constant and T is the temperature. An approximate initial density matrix $\hat{\rho}(0)$ is obtained by minimizing

$$\tilde{\Lambda} = \|\mathbf{m} - \mathbf{m}_B\|^2 + \lambda [\text{Tr}\{\mathbf{m} \mathbf{m}^\dagger\} - 1], \quad (45)$$

where \mathbf{m}_B is a square root of $\hat{\rho}_B$. This minimization is equivalent to a two-step procedure: first, maximizing $\text{Tr}\{\hat{\rho}_B \hat{P}_{N_b}\}$ with respect to the parameters of the basis, and second, constructing the initial density in the optimized basis as $\hat{\rho}(0) = \hat{P}_{N_b} \hat{\rho}_B \hat{P}_{N_b} / \text{Tr}\{\hat{\rho}_B \hat{P}_{N_b}\}$.

Solving the EOM (28-31) requires inversion of the \mathbf{S} and \mathbf{C} matrices, these matrices can become singular and lead to numerical difficulties.³³ This problem is addressed by applying a regularization procedure³⁴ on singular eigenvalues (s) before the matrix inversion: $s \rightarrow s + \varepsilon e^{-s/\varepsilon}$, where $\varepsilon = 10^{-6}$ is the chosen threshold. This procedure provides a faster and more stable propagation with a numerical precision of the order of ε . The limiting step of our implementation is the inversion of the \mathbf{C} matrix. The computational cost of this inversion scales cubically with the dimensionality of \mathbf{C} . For the system

with d DOF described by N_b Gaussians, the dimensionality of \mathcal{C} is $2N_b d$ (where the factor of two accounts for position and momentum parameters of Gaussians), and thus the computational cost scales as $8N_b^3 d^3$.

Simulations with time-dependent basis are compared with exact simulations that are done by projecting the QME onto the direct-product basis of the two-dimensional harmonic oscillator. 360 static basis functions are employed to obtain converged results that we will denote as $\hat{\rho}_e(t)$.

C. Isolated system simulations

For an isolated system where $h_1 = h_2 = 0$, $\mathcal{L}[\hat{\rho}] = -i[\hat{H}, \hat{\rho}]$, and $\mathcal{K}[\mathbf{m}] = -i\hat{H}\mathbf{m}$, we choose the temperature of the initial Boltzmann distribution to be $T = 1000$ K (or $T = 0.47\omega_1 = 0.41\omega_2$). Figure 1 shows population dynamics of the donor state, $\text{Tr}\{\hat{\rho}\hat{P}_D\}$, simulated with the NOSSE-based formalism. A good agreement with the exact propagation is obtained already for 25 CSs, and results of our method converges to those of the exact propagation with 35 CSs. Root-mean-square deviations (RMSDs) from the exact dynamics for various properties are defined as

$$\text{RMSD}(A) = \sqrt{\frac{1}{t_f} \int_0^{t_f} dt \text{Tr}\{\hat{A}[\hat{\rho}(t) - \hat{\rho}_e(t)]^2\}}, \quad (46)$$

where $t_f = 100$ fs, and $\hat{A} = \hat{1}$, \hat{P}_D , and \hat{H} for the total population (P_T), the donor state population (P_D), and the system energy (E), respectively. Table I shows that the system energy in QME-based simulations is not well conserved. As a result, the corresponding donor population dynamics have larger deviations than those in the NOSSE formalism.

The coupling between two electronic states is relatively weak and the population dynamics can be analyzed using perturbation theory. Fast scale oscillations are produced from transitions between $(m, n)_D$ and $(m, n \pm 1)_A$ levels due to the linear coupling [$c\hat{x}_2$ in Eq. (35)], here, the first and the second numbers correspond to the numbers of vibrational quanta along the tuning (x_1) and coupling (x_2) modes, and the subscripts denote the electronic states. Vibrational levels $(m, n)_D$ and $(m, n \pm 1)_A$ are separated

TABLE I. RMSDs of the donor population and energy with the NOSSE and QME approaches for different number N_b of CSs.

N_b	15	25	35
	RMSD(E), in units of ω_1		
NOSSE	$< 10^{-5}$	$< 10^{-5}$	$< 10^{-5}$
QME	$2.8 \cdot 10^{-3}$	$2.3 \cdot 10^{-3}$	$2.4 \cdot 10^{-3}$
	RMSD(P_D)		
NOSSE	$5.9 \cdot 10^{-3}$	$1.1 \cdot 10^{-3}$	$1.7 \cdot 10^{-4}$
QME	$6.1 \cdot 10^{-3}$	$1.1 \cdot 10^{-3}$	$4.9 \cdot 10^{-4}$

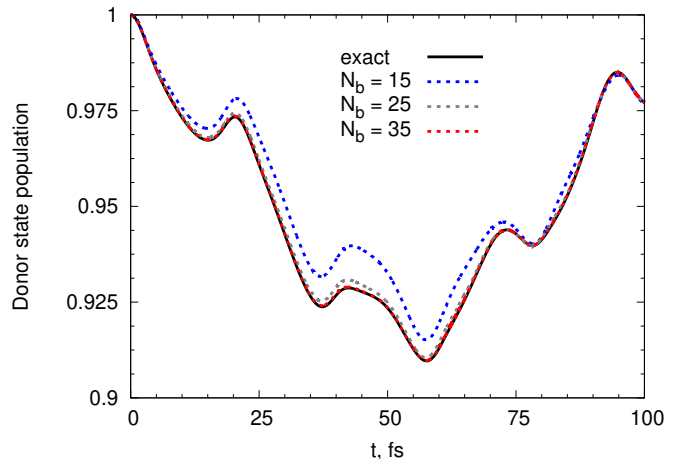


FIG. 1. Isolated system: Population dynamics of the donor electronic state $\text{Tr}\{\hat{\rho}(t)\hat{P}_D\}$ for the exact and vMCG dynamics based on constrained NOSSE [Eqs. (29) and (30)] formalism with different number N_b of CSs.

by the energy difference $\pm\omega_2$, which translates into the population oscillation period $t_p = 2\pi/\omega_2 = 23$ fs. There are also slower time-scale oscillations that appears as a result of transitions between the $(m, n)_D$ and $(m \mp 1, n \pm 1)_A$ levels. The tuning mode does not contribute to the coupling between electronic states, but it shifts minima of these states so that levels' couplings are modulated by the Franck-Condon factors. The energy difference between the $(m, n)_D$ and $(m \mp 1, n \pm 1)_A$ levels is $\pm(\omega_1 - \omega_2)$ that results in 143 fs time difference between two subsequent maxima of slow population oscillations.

D. Open system simulations

We simulate the system ($T = 1000$ K) located in the donor well and interacting with a harmonic bath according to Eq. (36) with $h_1 = 0$ and $h_2 = 3.675 \cdot 10^{-4}$ a.u. For $h_2 \neq 0$ the trace of $\hat{\rho}$ varies if no constraints are applied [see Eq. (43)]. In the constrained NOSSE-based vMCG simulations, the system density trace is conserved up to $2 \cdot 10^{-5}$. The population dynamics of the donor state $\text{Tr}\{\hat{\rho}(t)\hat{P}_D\}$ is given in Fig. 2, it illustrates that the constrained NOSSE vMCG formalism gives the exact dynamics for 35 CSs. A comparison of deviations from the exact dynamics in trace-constrained and unconstrained NOSSE simulations is given in Table II. As expected, the unconstrained NOSSE donor populations have larger deviations than those of the constrained formalism. Although generally there is no notable computational cost difference between constrained and unconstrained schemes, in some cases the constrained scheme has better efficiency due to more regularly behaving solutions of the corresponding EOM. Thus, all open system calculations similar to the ones reported here should be done with the constrained formalism.

The fast-scale oscillations (23 fs period) observed in the

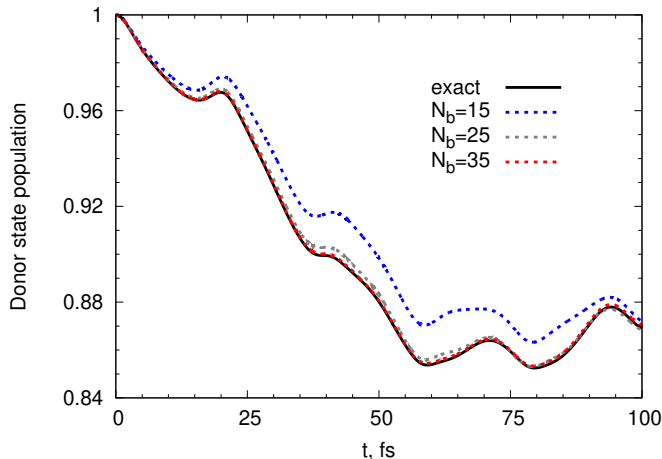


FIG. 2. Open system: Population dynamics of the donor electronic state $\text{Tr}\{\hat{\rho}(t)\hat{P}_D\}$ for the exact and vMCG dynamics based on constrained NOSSE [Eqs. (29) and (30)] formalism with different number N_b of CSs.

isolated system case are also present in Fig. 2, and their nature is exactly the same. However, due to influence of the environment, the long term dynamics has changed in the open system case. The origin of the irreversible decay of the donor population is a two-step-resonance process: $(0, 0)_D \rightarrow (0, 1)_D \rightarrow (0, 0)_A$, where the first step is driven by the environment excitation of the system within the donor state, while the second step is due to the linear coupling between the electronic states. Since there is no energy difference between the initial $(0, 0)_D$ and the final $(0, 0)_A$ states, this process leads to the larger population transfer observed in Fig. 2.

IV. CONCLUDING REMARKS

In this work we exposed the energy and total population non-conservation problems that occur in the density matrix TDVP formalism. The proposed constrained TDVP-NOSSE approach resolves the non-conservation issues by combining the Lagrange multiplier method to preserve the total population and the NOSSE formalism to reproduce unitary dynamics in the isolated system limit. As illustrated on a model surface-crossing

TABLE II. RMSDs of the total and donor populations with the constrained and unconstrained NOSSE approaches for different number N_b of CSs.

N_b	15	25	35
RMSD(P_T)			
Constrained	$< 10^{-5}$	$< 10^{-5}$	$< 10^{-5}$
Unconstrained	$8.8 \cdot 10^{-2}$	$2.2 \cdot 10^{-2}$	$6.5 \cdot 10^{-3}$
RMSD(P_D)			
Constrained	$1.3 \cdot 10^{-2}$	$1.9 \cdot 10^{-3}$	$6.2 \cdot 10^{-4}$
Unconstrained	$6.8 \cdot 10^{-2}$	$1.8 \cdot 10^{-2}$	$5.0 \cdot 10^{-3}$

problem, the developed approach can significantly reduce the number of propagated parameters for simulating non-adiabatic dynamics while conserving all required physical quantities. Moreover, even larger efficiency improvements compare to standard techniques are expected in molecular problems with a large number of nuclear DOF. Although the current implementation of the constrained TDVP-NOSSE approach has been illustrated using vMCG ansatz, working equations can be easily used to derive other system density parametrizations (e.g., MCTDH). For a better numerical stability we have used a basis of CSs that are localized in space. Thus our implementation is perfectly suited for a combination with the on-the-fly evaluation of electronic potential energy surfaces.^{32,35,36} From the application prospective, our developments open a new venue of the on-the-fly photochemistry with incoherent light. The sun light is incoherent, hence, realistic modelling of chemical photostability, solar energy harvesting and utilization requires introducing light as the system environment in a mixed state, which can be easily handled by the current approach.

ACKNOWLEDGEMENTS

L.J.D. thanks Ilya Ryabinkin for useful discussions and the European Union Seventh Framework Programme (FP7/2007-2013) for financial support under grant agreement PIOF-GA-2012-332233. A.F.I. acknowledges funding from the Natural Sciences and Engineering Research Council of Canada (NSERC) through the Discovery Grants Program.

V. APPENDIX: DERIVATION OF THE EQUATIONS OF MOTION FOR THE TDVP APPLIED TO QME

Main steps in derivation of Eqs. (7) - (11) are detailed below. Considering the parameterization of the DM in Eq. (4), variation of $\delta\hat{\rho}$ in Eq. (6) can be split into contributions from B_{kl} , $z_{\alpha k}$, and $z_{\alpha k}^*$

$$\delta\hat{\rho} = \sum_{kl} \frac{\partial\hat{\rho}}{\partial B_{kl}} \delta B_{kl} + \sum_{k\alpha} \left[\frac{\partial\hat{\rho}}{\partial z_{\alpha k}} \delta z_{\alpha k} + \frac{\partial\hat{\rho}}{\partial z_{\alpha k}^*} \delta z_{\alpha k}^* \right]. \quad (47)$$

Owing to independent character of δB_{kl} , $\delta z_{\alpha k}$, and $\delta z_{\alpha k}^*$ variations in Eq. (47), Eq. (6) represents a system of equations

$$\text{Tr} \left\{ \frac{\partial\hat{\rho}}{\partial B_{kl}} \left(\dot{\hat{\rho}} - \mathcal{L}[\hat{\rho}] \right) \right\} = 0, \quad (48)$$

$$\text{Tr} \left\{ \frac{\partial\hat{\rho}}{\partial z_{\alpha k}} \left(\dot{\hat{\rho}} - \mathcal{L}[\hat{\rho}] \right) \right\} = 0, \quad (49)$$

$$\text{Tr} \left\{ \frac{\partial\hat{\rho}}{\partial z_{\alpha k}^*} \left(\dot{\hat{\rho}} - \mathcal{L}[\hat{\rho}] \right) \right\} = 0. \quad (50)$$

Replacing $\hat{\rho}$ by its explicit form [Eq. (4)] into Eq. (48) leads to

$$\begin{aligned} & \sum_{ab} \frac{\partial B_{ba}}{\partial B_{kl}} \langle \varphi_b | \left\{ \sum_{cd} \left(|\varphi_c\rangle \dot{B}_{cd} \langle \varphi_d | + |\dot{\varphi}_c\rangle B_{cd} \langle \varphi_d | \right. \right. \\ & \quad \left. \left. + |\varphi_c\rangle B_{cd} \langle \dot{\varphi}_d | \right) - \mathcal{L}[\hat{\rho}] \right\} | \varphi_a \rangle \\ & = \sum_{cd} \left(S_{kc} \dot{B}_{cd} S_{dl} + \tau_{kc} B_{cd} S_{dl} + S_{kc} B_{cd} \tau_{ld}^* \right) - L_{kl} = 0, \end{aligned} \quad (51)$$

where $S_{kc} = \langle \varphi_k | \varphi_c \rangle$ is the overlap matrix between time-dependent basis functions, $\tau_{kc} = \langle \varphi_k | \dot{\varphi}_c \rangle$, and $L_{kl} = \langle \varphi_k | \mathcal{L}[\hat{\rho}] | \varphi_l \rangle$. Using the matrix notation, Eq. (51) is completely equivalent to Eq. (7).

Equations (49) and (50) are complex conjugates of each other, and therefore, constitute one unique stationary condition. Replacing $\hat{\rho}$ by its explicit form [Eq. (4)] into Eq. (49) leads to

$$\sum_{ab} B_{ab} \left\langle \frac{\partial \varphi_b}{\partial z_{\alpha k}} \right| \left\{ \sum_{cd} \left(|\dot{\varphi}_c\rangle B_{cd} \langle \varphi_d | + |\varphi_c\rangle B_{cd} \langle \dot{\varphi}_d | \right. \right. \\ \left. \left. + |\varphi_c\rangle \dot{B}_{cd} \langle \varphi_d | \right) - \mathcal{L}[\hat{\rho}] \right\} | \varphi_a \rangle = 0.$$

Substituting \dot{B}_{cd} by Eq. (7) we obtain

$$\begin{aligned} & \sum_a \left\langle \frac{\partial \varphi_k}{\partial z_{\alpha k}} \right| \left\{ \sum_{cd} \left(|\dot{\varphi}_c\rangle B_{cd} S_{da} + |\varphi_c\rangle B_{cd} \langle \dot{\varphi}_d | \varphi_a \rangle \right. \right. \\ & \quad \left. \left. + |\varphi_c\rangle [S^{-1} L S^{-1} - S^{-1} \tau B - B \tau^\dagger S^{-1}]_{cd} S_{da} \right) \right. \\ & \quad \left. - \mathcal{L}[\hat{\rho}] | \varphi_a \rangle \right\} B_{ak} \\ & = \sum_a \left\langle \frac{\partial \varphi_k}{\partial z_{\alpha k}} \right| \left\{ \sum_{cd} (\hat{1} - \hat{P}_{N_b}) |\dot{\varphi}_c\rangle B_{cd} S_{da} \right. \\ & \quad \left. + (\hat{P}_{N_b} - \hat{1}) \mathcal{L}[\hat{\rho}] | \varphi_a \rangle \right\} B_{ak} \\ & = 0, \end{aligned} \quad (52)$$

where we used the definition of the projector $\hat{P}_{N_b} = \sum_{kl} |\varphi_k\rangle [S^{-1}]_{kl} \langle \varphi_l |$. The time derivative in Eq. (52) can be expanded using the chain rule in terms of the basis set parameters $\partial/\partial t = \sum_{l\beta} \dot{z}_{l\beta} \partial/\partial z_{l\beta}$, thus

$$\begin{aligned} & \sum_{l\beta} \left\langle \frac{\partial \varphi_k}{\partial z_{\alpha k}} \right| \left[\hat{1} - \hat{P}_{N_b} \right] \left| \frac{\partial \varphi_l}{\partial z_{l\beta}} \right\rangle [\mathbf{B} \mathbf{S} \mathbf{B}]_{lk} \dot{z}_{l\beta} \\ & \quad - \left\langle \frac{\partial \varphi_k}{\partial z_{\alpha k}} \right| \left[\hat{1} - \hat{P}_{N_b} \right] \mathcal{L}[\hat{\rho}] | \varphi_l \rangle [\mathbf{B}]_{lk} \\ & = \sum_{l\beta} \tilde{C}_{kl}^{\alpha\beta} \dot{z}_{l\beta} - \tilde{Y}_k^\alpha = 0, \end{aligned} \quad (53)$$

that is Eq. (8) with definitions given in Eqs. (9) and (10).

VI. APPENDIX: DERIVATION OF THE EQUATIONS OF MOTION FOR THE CONSTRAINED TDVP APPLIED TO NOSSE

Here we provide main steps in derivation of Eqs. (27) - (30). Starting from the constrained TDVP Eq. (25) we

note that variations

$$\delta \dot{\mathbf{m}}^\dagger = \sum_{kl} \frac{\partial \mathbf{m}^\dagger}{\partial M_{kl}^*} \delta \dot{M}_{kl}^* + \sum_{k\alpha} \frac{\partial \mathbf{m}^\dagger}{\partial z_{\alpha k}^*} \delta z_{\alpha k}^* \quad (54)$$

and

$$\delta \mathbf{m}^\dagger = \sum_{kl} \frac{\partial \mathbf{m}^\dagger}{\partial M_{kl}^*} \delta M_{kl}^* + \sum_{k\alpha} \frac{\partial \mathbf{m}^\dagger}{\partial z_{\alpha k}^*} \delta z_{\alpha k}^* \quad (55)$$

span the same tangent space of $\mathbf{m}(t)$ because variations of parameters (δM_{kl}^* , $\delta z_{\alpha k}^*$) and their time derivatives ($\delta \dot{M}_{kl}^*$, $\delta \dot{z}_{\alpha k}^*$) are completely arbitrary. Therefore, Eq. (25) can be substituted as

$$\text{Re} [\text{Tr} \{ \delta \mathbf{m}^\dagger (\dot{\mathbf{m}} - \mathcal{K}[\mathbf{m}] + \lambda \mathbf{m}) \}] = 0. \quad (56)$$

The parameterization of $\mathbf{m}(t)$ is chosen so that the basis functions $|\varphi_k\rangle$ are analytic with respect to their parameters, $\partial |\varphi_k\rangle / \partial z_{\alpha k}^* = 0$. This analyticity allows us to extend the zero condition in Eq. (56) from a real part to the total trace expression²²

$$\text{Tr} \{ \delta \mathbf{m}^\dagger (\dot{\mathbf{m}} - \mathcal{K}[\mathbf{m}] + \lambda \mathbf{m}) \} = 0. \quad (57)$$

The variation $\delta \mathbf{m}^\dagger$ is split into contribution from M_{kl} and $z_{\alpha k}$ [Eq. (55)], and using independence and arbitrariness of variations for different parameters, Eq. (57) is rewritten as a set of equations

$$\text{Tr} \left\{ \frac{\partial \mathbf{m}^\dagger}{\partial M_{kl}^*} (\dot{\mathbf{m}} - \mathcal{K}[\mathbf{m}] + \lambda \mathbf{m}) \right\} = 0, \quad (58)$$

$$\text{Tr} \left\{ \frac{\partial \mathbf{m}^\dagger}{\partial z_{\alpha k}^*} (\dot{\mathbf{m}} - \mathcal{K}[\mathbf{m}] + \lambda \mathbf{m}) \right\} = 0. \quad (59)$$

Replacing \mathbf{m}^\dagger by its explicit form [Eq. (20)] in Eq. (58) leads to

$$\begin{aligned} & \sum_{ab} \frac{\partial M_{ba}^*}{\partial M_{kl}^*} \langle \varphi_b | \left\{ \sum_c \left(|\varphi_c\rangle \dot{M}_{ca} + |\dot{\varphi}_c\rangle M_{ca} \right. \right. \\ & \quad \left. \left. + \lambda |\varphi_c\rangle M_{ca} \right) - |\mathcal{K}_a[\mathbf{m}] \rangle \right\} \\ & = \sum_c \left(S_{kc} \dot{M}_{cl} + \tau_{kc} M_{cl} + \lambda S_{kc} M_{cl} \right) - K_{kl} = 0, \end{aligned} \quad (60)$$

or using a matrix notation for Eq. (60) gives

$$\dot{\mathbf{M}} = \mathbf{S}^{-1} \mathbf{K} - \mathbf{S}^{-1} \boldsymbol{\tau} \mathbf{M} - \lambda \mathbf{M}. \quad (61)$$

Inserting Eq. (61) into the constraint Eq. (26) gives the expression of the Lagrange multiplier

$$\begin{aligned} \lambda & = \frac{\text{Tr} \{ \mathbf{M} \mathbf{K}^\dagger + \mathbf{K} \mathbf{M}^\dagger \}}{2 \text{Tr} \{ \mathbf{M}^\dagger \mathbf{S} \mathbf{M} \}} \\ & = \frac{1}{2} \text{Tr} \{ \mathbf{M} \mathbf{K}^\dagger + \mathbf{K} \mathbf{M}^\dagger \}, \end{aligned} \quad (62)$$

where the second equality arises because the $\text{Tr} \{ \mathbf{M}^\dagger \mathbf{S} \mathbf{M} \} = \text{Tr} \{ \mathbf{m} \mathbf{m}^\dagger \} = \text{Tr} \{ \hat{\rho} \} = 1$. Substituting λ by Eq. (62) in Eq. (61) leads to the final equation of motion for \mathbf{M} [Eq. (27)].

To derive the EOM for $z_{\alpha k}$ we replace \mathbf{m}^\dagger by its explicit form [Eq. (20)] in Eq. (59)

$$\sum_{ab} M_{ba}^* \left\langle \frac{\partial \varphi_b}{\partial z_{\alpha k}} \left| \left\{ \sum_c (|\varphi_c\rangle \dot{M}_{ca} + |\dot{\varphi}_c\rangle M_{ca} + \lambda |\varphi_c\rangle M_{ca}) - |\mathcal{K}_a[\mathbf{m}]\rangle \right\} \right. \right\rangle = 0. \quad (63)$$

Substituting \dot{M}_{ca} by Eq. (61) gives

$$\begin{aligned} & \sum_a M_{ka}^* \left\langle \frac{\partial \varphi_k}{\partial z_{\alpha k}} \left| \left\{ \sum_c (|\varphi_c\rangle [\mathbf{S}^{-1} \mathbf{K} - \mathbf{S}^{-1} \boldsymbol{\tau} \mathbf{M} - \lambda \mathbf{M}]_{ca} + |\dot{\varphi}_c\rangle M_{ca} + \lambda |\varphi_c\rangle M_{ca}) - |\mathcal{K}_a[\mathbf{m}]\rangle \right\} \right. \right\rangle \\ &= \sum_a \left\langle \frac{\partial \varphi_k}{\partial z_{\alpha k}} \left| \left\{ \sum_c (\hat{1} - \hat{P}_{N_b}) |\dot{\varphi}_c\rangle M_{ca} + (\hat{P}_{N_b} - 1) |\mathcal{K}_a[\mathbf{m}]\rangle \right\} M_{ka}^* \right. \right\rangle \\ &= 0. \end{aligned} \quad (64)$$

Expanding the time derivative using the chain rule in terms of the basis set parameters gives

$$\begin{aligned} & \sum_{l\beta} \left\langle \frac{\partial \varphi_k}{\partial z_{\alpha k}} \left| \left[\hat{1} - \hat{P}_{N_b} \right] \left| \frac{\partial \varphi_l}{\partial z_{l\beta}} \right\rangle [\mathbf{M} \mathbf{M}^\dagger]_{lk} \dot{z}_{l\beta} \right. \\ & \quad \left. - \sum_l \left\langle \frac{\partial \varphi_k}{\partial z_{\alpha k}} \left| \left[\hat{1} - \hat{P}_{N_b} \right] |\mathcal{K}_l[\mathbf{m}]\rangle M_{kl}^* \right. \right\rangle \right. \\ & \left. = \sum_{l\beta} C_{kl}^{\alpha\beta} \dot{z}_{l\beta} - Y_k^\alpha = 0, \end{aligned} \quad (65)$$

where we used the definitions from Eqs. (29) and (30). Adopting the matrix notation the last equation can be rewritten as Eq. (28).

¹E. Collini, C. Wong, K. Wilk, P. Curmi, P. Brumer, and G. Scholes, *Nature* **463**, 644 (2010).

²M. Boggio-Pasqua, M. A. Robb, and G. Groenhof, *J. Am. Chem. Soc.* **131**, 13580 (2009).

³P. Kukura, D. W. McCamant, S. Yoon, D. B. Wandschneider, and R. A. Mathies, *Science* **310**, 1006 (2005).

⁴P. A. M. Dirac, in *The Principles of Quantum Mechanics, 4th Edition* (Clarendon Press, Oxford, 1958) p. 125.

⁵J. Frenkel, in *Wave Mechanics* (Clarendon Press, Oxford, 1934) p. 253.

⁶A. McLachlan, *Mol. Phys.* **8**, 39 (1964).

⁷M. Beck, A. Jäckle, G. Worth, and H.-D. Meyer, *Phys. Rep.* **324**, 1 (2000).

⁸I. Burghardt, H.-D. Meyer, and L. S. Cederbaum, *J. Chem. Phys.* **111**, 2927 (1999).

⁹H. Wang and M. Thoss, *J. Chem. Phys.* **119**, 1289 (2003).

¹⁰G. A. Worth, M. A. Robb, and I. Burghardt, *Farad. Discuss.* **127**, 307 (2004).

¹¹A. F. Izmaylov, *J. Chem. Phys.* **138**, 104115 (2013).

¹²T. V. Tscherbul and P. Brumer, *J. Phys. Chem. A* **118**, 3100 (2014).

¹³H.-P. Breuer and F. Petruccione, eds., *The Theory of Open Quantum Systems* (Oxford University Press, New York, 2002).

¹⁴A. Nitzan, *Chemical dynamics in condensed phase* (Oxford University Press, NY, 2006) pp. 084502–084502–9.

¹⁵G. Lindblad, *Commun. Math. Phys.* **48**, 119 (1976).

¹⁶A. G. Redfield, *Adv. Magn. Reson.* **1**, 1 (1965).

¹⁷A. O. Caldeira and A. J. Leggett, *Physica A* **121**, 587 (1983).

¹⁸T. Gerdtts and U. Manthe, *J. Chem. Phys.* **106**, 3017 (1997).

¹⁹A. Raab, I. Burghardt, and H.-D. Meyer, *J. Chem. Phys.* **111**, 8759 (1999).

²⁰A. Raab and H.-D. Meyer, *Theor. Chem. Acc.* **104**, 358 (2000).

²¹E. J. Heller, *J. Chem. Phys.* **64**, 63 (1976).

²²J. Broeckhove, L. Lathouwers, E. Kesteloot, and P. Van Leuven, *Chem. Phys. Lett.* **149**, 547 (1988).

²³K.-K. Kan, *Phys. Rev. A* **24**, 2831 (1981).

²⁴L. Joubert-Doriol and A. F. Izmaylov, Supplemental material.

²⁵L. Joubert-Doriol, I. G. Ryabinkin, and A. F. Izmaylov, *J. Chem. Phys.* **141**, 234112 (2014).

²⁶H. Köppel, W. Domcke, and L. S. Cederbaum, “Multimode Molecular Dynamics Beyond the Born-Oppenheimer Approximation,” (John Wiley & Sons, Inc., 1984) Chap. 2, pp. 59–246.

²⁷A. Migani and M. Olivucci, in *Conical Intersection Electronic Structure, Dynamics and Spectroscopy*, edited by W. Domcke, D. R. Yarkony, and H. Köppel (World Scientific, New Jersey, 2004) p. 271.

²⁸W. Domcke and D. R. Yarkony, *Annu. Rev. Phys. Chem.* **63**, 325 (2012).

²⁹I. G. Ryabinkin, L. Joubert-Doriol, and A. F. Izmaylov, *J. Chem. Phys.* **140**, 214116 (2014).

³⁰T. Takagahara, E. Hanamura, and R. Kubo, *J. Phys. Soc. Japan* **44**, 728 (1978).

³¹B. Wolfseder and W. Domcke, *Chem. Phys. Lett.* **235**, 370 (1995).

³²K. Saita and D. V. Shalashilin, *J. Chem. Phys.* **137**, 22A506 (2012).

³³I. Burghardt, M. Nest, and G. A. Worth, *J. Chem. Phys.* **119**, 5364 (2003).

³⁴H.-D. Meyer, F. Gatti, and G. A. Worth, eds., *Multidimensional Quantum Dynamics: MCTDH Theory and Applications* (Wiley-VCH, Weinheim, 2009).

³⁵M. Ben-Nun, J. Quenneville, and T. J. Martinez, *J. Phys. Chem. A* **104**, 5161 (2000).

³⁶G. Worth, M. Robb, and B. Lasorne, *Mol. Phys.* **106**, 2077 (2008).